ELSEVIER

Epilepsy Research 44 (2001) 129–140

Epilepsy Research

www.elsevier.com/locate/epilepsyres

# The epileptic process as nonlinear deterministic dynamics in a stochastic environment: an evaluation on mesial temporal lobe epilepsy

R.G. Andrzejak [a,b,*], G. Widman [a], K. Lehnertz [a], C. Rieke [a,b], P. David [b], C.E. Elger [a]

[a] *Department of Epileptology, Medical Center, University of Bonn, Sigmund Freud Str. 25, 53105 Bonn, Germany*
[b] *Institut für Strahlen und Kernphysik, University of Bonn, Bonn, Germany*

Received 10 October 2000; received in revised form 15 January 2001; accepted 19 January 2001

**Abstract**

The theory of deterministic chaos addresses simple deterministic dynamics in which nonlinearity gives rise to complex temporal behavior. Although biological neuronal networks such as the brain are highly complicated, a number of studies provide growing evidence that nonlinear time series analysis of brain electrical activity in patients with epilepsy is capable of providing potentially useful diagnostic information. In the present study, this analysis framework was extended by introducing a new measure $\xi$, designed to discriminate between nonlinear deterministic and linear stochastic dynamics. For the evaluation of its discriminative power, $\xi$ was extracted from intracranial multi-channel EEGs recorded during the interictal state in 25 patients with unilateral mesial temporal lobe epilepsy. Strong indications of nonlinear determinism were found in recordings from within the epileptogenic zone, while EEG signals from other sites mainly resembled linear stochastic dynamics. In all investigated cases, this differentiation allowed to retrospectively determine the side of the epileptogenic zone in full agreement with results of the presurgical workup. 

*Keywords:* Nonlinear determinism; Epileptogenic zone; Mesial temporal lobe epilepsy; EEG

## 1. Introduction

A general concept in science is the characterization of dynamical systems from the analysis of variables evolving in time, such as the EEG. In epileptology, analyses of intracranial EEG recordings are generally considered valuable for a characterization of the spatio-temporal dynamics of the epileptogenic process. While the expert's visual inspection of both the ictal and interictal EEG morphology, frequency and amplitude is still the standard for focus localization, computerized EEG analysis methods have obtained increas-

* Corresponding author. Tel.: +49-228-2875864; fax: +49-228-2876294.
*E-mail address:* ralphandrzejak@yahoo.de (R.G. Andrzejak).

0920-1211/01/$ - see front matter 
PII: S0920-1211(01)00195-4

ing attention in the past few decades (Lopes da Silva et al., 1986; Alarcon et al., 1997). A rich literature deals with the extraction of measures based on power spectral estimates (Gersch and Goddard, 1970; Nuwer, 1988; Panet-Raymond and Gotman, 1990; Marciani et al., 1992; Alarcon et al., 1995; Drake et al., 1998). The ability of this measure to discriminate between deterministic and stochastic dynamics, however, is confined to linear systems, i.e. systems in which cause and effect are proportional. Deterministic dynamics can be distinguished from stochastic dynamics by the existence of an unambiguous relation between present and future states. Because the dynamical behavior of individual neurons is governed by threshold and saturation properties, nonlinearity is introduced to neuronal networks already on the cellular level. Even in simple deterministic dynamical systems, nonlinearity can give rise to erratic and aperiodic behavior that appears to be stochastic within the scope of power spectral analysis methods. Comprehension of such complex dynamical systems can be achieved with the help of concepts of deterministic chaos (Schuster, 1989). Within this framework, nonlinear time series analysis (NTSA) offers a variety of algorithms and measures, each extracting different dynamical features from the underlying dynamical system (Kantz and Schreiber, 1997).

Though neuronal networks are doubtlessly much more complicated than those systems for which NTSA was originally developed, a number of authors have investigated whether the application of these techniques to the EEG can reveal traits of neuronal dynamics. In early studies, low values of the correlation dimension and positive values of the largest Lyapunov exponent (LLE), calculated from scalp EEG recordings during epileptic seizures, were interpreted as evidence for underlying chaotic and thereby deterministic dynamics (e.g. Babloyantz and Destexhe, 1986; Frank et al., 1990). Iasemides et al. (1990) extracted LLE from EEGs recorded with intracranial subdural electrodes in a patient with temporal lobe epilepsy during the peri-ictal state. Authors concluded that the reported 'change in chaoticity' traced by the spatio-temporal LLE profiles might be useful to detect onset and spatial spread of ictal discharges. In the following years, a number of authors questioned the evidence of deterministic chaos data by discussing and re-examining the probative force of absolute values of NTSA-measures (Theiler, 1995; Theiler and Rapp, 1996; Schreiber, 2000). Investigating peri-ictal EEGs recorded intracranially in kindled rats Pijn et al. (1991) were the first to calculate the correlation sum for both the EEG and stochastic control signals. Their method of constructing stochastic control signals was later generalized to the concept of surrogate data (Theiler et al., 1992).

In more recent studies, a number of authors have pursued the idea that NTSA might contribute to a spatial characterization of the epileptogenic process even during the interictal state. Lehnertz and Elger (1995) and Weber et al. (1998) successfully lateralized the epileptogenic zone (Lüders and Awad, 1991) in larger groups of patients with unilateral temporal lobe epilepsy extracting a complexity measure based on an effective correlation dimension from invasive or semi-invasive EEG recordings. Widman et al. (2000) recently demonstrated the applicability of this method to neocortical lesional epilepsies. Investigating the detectability of nonlinearity, Casdagli et al. (1997) used the correlation sum exclusively as statistics for a surrogate test and refrained from any further evaluations concerning finite or infinite dimension (cf. Rombouts et al., 1995). For two patients with mesial temporal lobe epilepsy, Casdagli et al. (1997) established prominent nonlinearities in signals recorded intracranially from the epileptogenic hippocampus and from interictal spike foci during the peri-ictal state.

The concept of the correlation sum and with it the correlation dimension is most appropriate for the analysis of deterministic dynamical systems (Kantz and Schreiber, 1995), whereas properties of stochastic dynamics, which are, in principle, of infinite dimension, may cause spurious detections of low dimensionality (Osborne and Provenzale, 1989; Rapp et al., 1993). Thus, the correlation dimension alone allows no unambiguous distinction between deterministic and stochastic dynamics. Different approaches were developed for a straightforward discrimination between nonlinear

deterministic and linear stochastic dynamics (e.g. Casdagli, 1989; Kaplan and Glass, 1992; Wayland et al., 1993; Salvino and Cawley, 1994; Kaplan, 1994). Applying these methods to brain electrical activity, several authors ruled out indications for nonlinear deterministic dynamics in scalp EEG recordings from healthy volunteers (Glass et al., 1993; Palus, 1994; Jeong et al., 1999). Comparing different tests for determinism as well as different types of surrogates, Schiff and Chang, 1992; Schiff et al. (1994) and Chang et al. (1994) analyzed data from several experimental animal models. Indications of nonlinear deterministic dynamics were found only in a small fraction of the investigated cases, including seizure-like activity in a rat hippocampal slice in an epilepsy model (Schiff et al. 1994). So et al. (1998) recently established indications of deterministic components by extracting unstable periodic orbits (So et al., 1997) from interspike intervals. These indications were found in intra- and extracellular measurements from rat hippocampal slices and in interictal spike intervals from an EEG recording in a patient with epilepsy. Interictal spikes, however, are known to represent an infrequent spatio-temporal phenomenon.

Based on the hypothesis that the epileptogenic process can be characterized as nonlinear deterministic dynamics in an otherwise linear stochastic environment of brain electrical activity, the measure $\xi$, which combines the methods of coarse-grained flow average (Kaplan and Glass, 1992) and improved surrogates (Schreiber and Schmitz, 1996), was specifically designed to be used as a straightforward test for nonlinear determinism. This test was applied to continuous intracranial EEG recordings of patients with mesial temporal lobe epilepsy to evaluate its merit for a spatial characterization of the epileptogenic process.

## 2. Methods

### 2.1. Patient characteristics

Twenty-five patients with pharmacoresistent mesial temporal lobe epilepsy (MTLE) were included in this retrospective study. The mean age of the 12 female and 13 male patients was $31 \pm 9$ years, ranging from 10 to 46 years. The age at onset of epilepsy was $11 \pm 9$ years, ranging from 0 to 36 years. All patients were evaluated for epilepsy surgery according to the Bonn protocol of presurgical evaluation (cf. Engel, 1993) and were diagnosed as having a unilateral mesial temporal seizure origin (16 left, nine right). Selective amygdalohippocampectomy led to post-operative complete seizure control in all cases, followed up for at least 2 years by our outpatient department. Histopathological evaluation of the resected brain tissue demonstrated hippocampal pathology with signs of atrophy and varying degrees of sclerosis in all patients.

### 2.2. Recording techniques

A total of 82 artifact-free electrocorticographic (ECoG) and stereoelectroencephalographic (SEEG) recordings were analyzed. Included in the study were all recordings that were archived during the pre-surgical work up and did not contain periods of ictal or post-ictal activity, hyperventilations or other seizure provocation techniques. The presence or absence of inter-ictal epileptiform activity or levels of anticonvulsive medication, however, did not serve as a selection criterion. Recording lengths varied from 20 to 220 min, with an average total length of 84 min per patient. The EEG was recorded under video control in an electrically shielded room using chronically implanted subdural and intrahippocampal depth electrodes (cf. Fig. 1). Subdural electrode contacts of 2.5 mm diameter consisted of stainless steel with an intercontact distance of 10 or 15 mm, respectively, depending on their cortical localization. Bilateral silastic depth electrodes of 1 mm thickness were implanted stereotactically via the longitudinal axis of the hippocampal formation using an occipital approach (cf. Spencer et al., 1993; Van Roost et al., 1998). Each electrode carried ten cylindrical contacts of a nickel-chromium alloy with a length of 2.5 mm and an intercontact distance of 4 mm. After implantation, correct electrode placement was verified using cranial computer tomography and magnet resonance imaging scans.

EEG signals were passed to a 128-channel amplifier system with band-pass filter settings of 0.53–85 Hz (12 dB/oct.) using a common average reference (omitting those electrodes which have been proven to contain obvious pathological activity during a pre-analysis). After 12-bit A/D conversion, the data for each channel was written continuously onto the disk of a data acquisition computer system at a sampling time of 5.76 ms.

### 2.3. Calculation of the estimate $\xi$

The measure $\xi$ is introduced in the present study in order to discriminate between nonlinear deterministic and linear stochastic dynamics. It is based on the coarse-grained flow average $\Lambda$ that aims to distinguish deterministic and stochastic dynamics (Kaplan and Glass, 1992). This measure quantifies the degree to which nearby segments of trajectories point to similar directions in a state space that is reconstructed using delay coordinates (Takens, 1981) and coarse grained into hypercubes. As already stressed by Kaplan and Glass (1992), it is essential to calculate $\Lambda$ for both the original time series and an ensemble of surrogate time series (Theiler et al., 1992; Schreiber and Schmitz, 1996). The latter are constructed to share certain linear properties with the original time series, but are otherwise random. For a detailed description of these techniques refer to Appendix A.

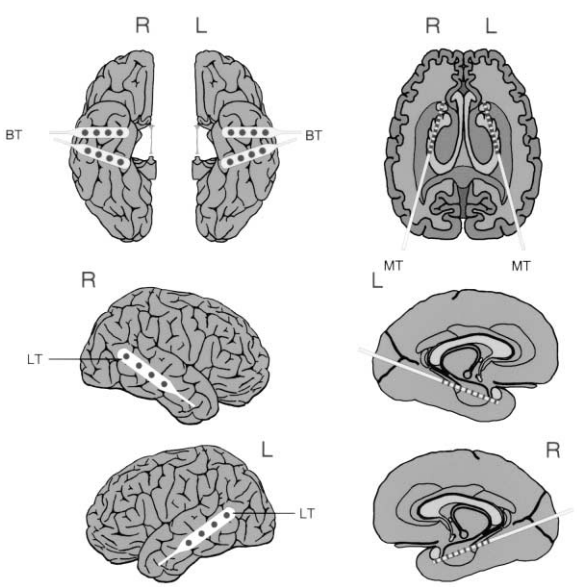


Fig. 1. Scheme of location of implanted subdural strip and intrahippocampal depth electrodes. Abbreviations: BT, basal temporal; LT, lateral temporal; MT, mesial temporal.

Both the calculation of $\Lambda$ and the generation of surrogate time series require stationarity of the dynamics under investigation. On the other hand, the length of the time series is essential to sufficiently cover the hypercubes with individual passes of the trajectory and thus, to reliably calculate $\Lambda$. As a compromise between these requirements, the length of EEG segments was set to 23.6 s (4096 data points). Discontinuities between the end and beginning of a time series are known to cause spurious frequency components in the power spectrum used for surrogate generation. To circumvent this problem, segments were cut out of longer epochs of 24.6 s length in a way that the amplitude difference between the last and first data point was within the range of amplitude differences of consecutive data points and the slopes at end and beginning of the time series had the same sign.

In order to maximally unfold and resolve unknown dynamics, high values of both the embedding dimension and the number of hypercubes should be chosen. However, given a restricted number of data points, the ranges of these two parameters are limited. If either exceeds reasonable values, a sufficient amount of trajectory passes through individual hypercubes again cannot be guaranteed. In consideration of these constraints, a pre-analysis showed that a sufficient number of passes through the hypercubes could be obtained for an embedding dimension of $m = 6$. The number of hypercubes $b$ was adjusted with respect to the analyzed time series. Depending on the quotient of the amplitude range and variance of the time series, $b$ values ranged from 6 to 20. This adaptation was necessary to ensure that occasional events with high amplitudes, such as spikes, do not lower the resolution of $\Lambda$.

The last parameter to be set was the reconstruction delay $\tau$. For small values of $\tau$, the trajectory is not unfolded but stretched out along the diagonal of the state space. An alignment of nearby

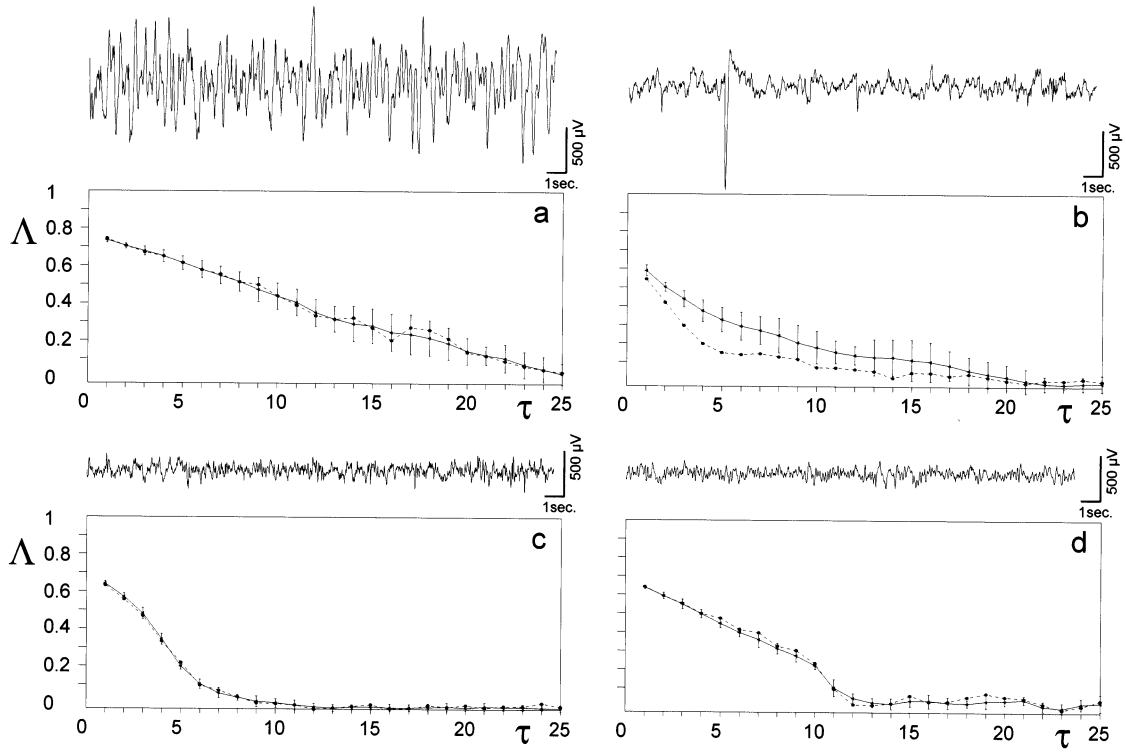


Fig. 2. Dependence of the coarse grained flow average $\Lambda$ on the reconstruction delay $\tau$ for selected EEG segments. The reconstruction delay is in units of the sampling time (5.76 ms). Dashed lines connect $\Lambda$ values calculated for the EEG, solid lines are used for mean values calculated from the surrogate ensemble. Error bars denote 2 S.D. Concordance within error bars of the two curves is established for (a), (c) and (d), corresponding to $\xi = 0$. For (b) the mean of the surrogate ensemble even exceeds values obtained for the EEG, also resulting in $\xi = 0$ (cf. Eq. (1)).

trajectory segments due to linear correlations is therefore predominant, causing high values of $\Lambda$ regardless of whether or not deterministic dynamics are present. On the other hand, high values of $\tau$ will lead to an overfolding of the trajectory, destroying a possible deterministic alignment of nearby trajectory segments. Rather than use a fixed value of the time delay, the estimate $\xi$ was therefore defined by summing over a range of delays:

$$\xi = \sum_{\tau=5}^{\tau=20} \Delta\Lambda(\tau)$$

where

$$\Delta\Lambda(\tau) = \begin{cases} \Lambda_{\mathrm{EEG}}(\tau) - \overline{\Lambda_{\mathrm{SUR}}(\tau)} & \text{if} \\ 0 & \text{else} \end{cases}$$

$$\Lambda_{\mathrm{EEG}}(\tau) > \overline{\Lambda_{\mathrm{SUR}}(\tau)} + 2\sigma(\Lambda_{\mathrm{SUR}}(\tau)) \quad (1)$$

The overbar denotes the mean of ten iterative amplitude-adjusted surrogates. Non-zero values of $\xi$ are obtained if and only if $\Lambda_{\mathrm{EEG}}(\tau)$ exceeds $\Lambda_{\mathrm{SUR}}(\tau)$ by $> 2$ S.D. for at least a subrange of the predefined reconstruction delay range. Values of $\xi$ from a moving-window-technique (50% overlap of consecutive windows) were first averaged over time for each electrode (cf. Figs. 1 and 4; notation $\langle \xi \rangle$). Subsequently, $\langle \xi \rangle$ values were averaged over electrodes belonging to the respective recording region (cf. Fig. 1; notation: $\overline{\xi}$).

## 3. Results

Detailed results for selected EEG windows (cf. Figs. 2 and 3) illustrate various degrees to which values of the coarse-grained flow average calculated for the EEG ($\Lambda_{EEG}(\tau)$) did deviate from the distribution calculated from the respective surrogate ensemble ($\Lambda_{SUR}(\tau)$).

For examples (a), (c) and (d) in Fig. 2, $\Lambda_{EEG}(\tau)$ is within 2 S.D. of the respective $\Lambda_{SUR}(\tau)$ distribution, corresponding to $\xi = 0$. Following Eq. (1), $\xi = 0$ also results for cases such as example (b) in Fig. 2, where $\Lambda_{SUR}(\tau)$ significantly exceeds $\Lambda_{EEG}(\tau)$. (cf. Fig. 3 and Eq. (1)). In contrast, all examples of Fig. 3 correspond to $\xi > 0$.

Results of $\xi$ analyses of an EEG recording (duration: 20 min) using a moving window are shown in Fig. 4. Apart from a high variability in time, a clear spatial gradient of $\xi$ is visible. On average, highest values were obtained for recordings from within or adjacent to the epileptogenic zone, i.e. the mesial temporal lobe.

Summarizing the results for all patients, mean values for the different recording locations are depicted in Fig. 5(a–c). First, a high inter-individual variability of $\overline{\xi}$ values is notable. Comparing only homologous recording regions for individual patients, higher $\overline{\xi}$ values were calculated for EEGs recorded from mesial temporal structures of the focal hemisphere in all investigated cases (cf. Fig. 5(a) and Table 1). On this basis, the epileptogenic zone could be lateralized correctly.

For those patients implanted with additional subdural strip electrodes, the comparison of homologous structures was extended to recording regions adjacent to (basal region) and remote from (lateral region) the epileptogenic zone. Here, higher $\overline{\xi}$ values were calculated for focal hemisphere in 15 of 17 (basal region) and in eight of 12 (lateral region) cases. Hence, the clear discrimination diminished with increased distance from the epileptogenic focus (cf. Fig. 5(b,c) and Table 1).

When the comparison was extended to differences in between $\overline{\xi}$ values obtained from non-ho-

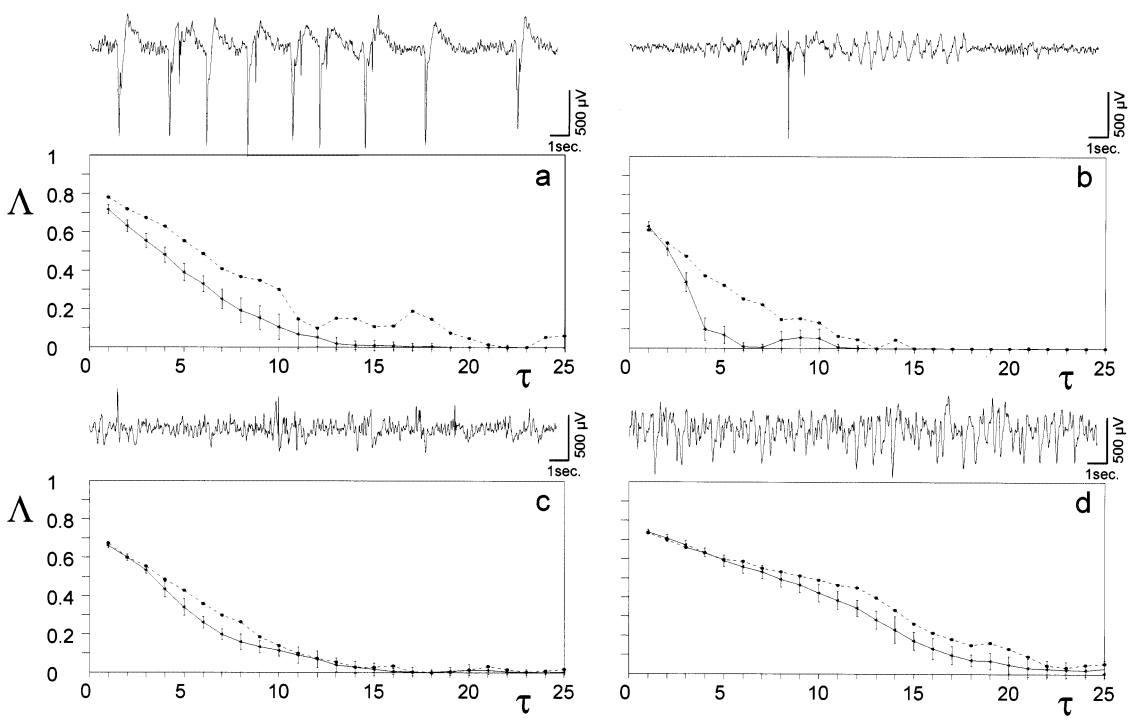


Fig. 3. Same as Fig. 2. For the examples given here, $\Lambda_{EEG}(\tau)$ exceeds from $\Lambda_{SUR}(\tau)$, corresponding to nonzero values of $\xi$.

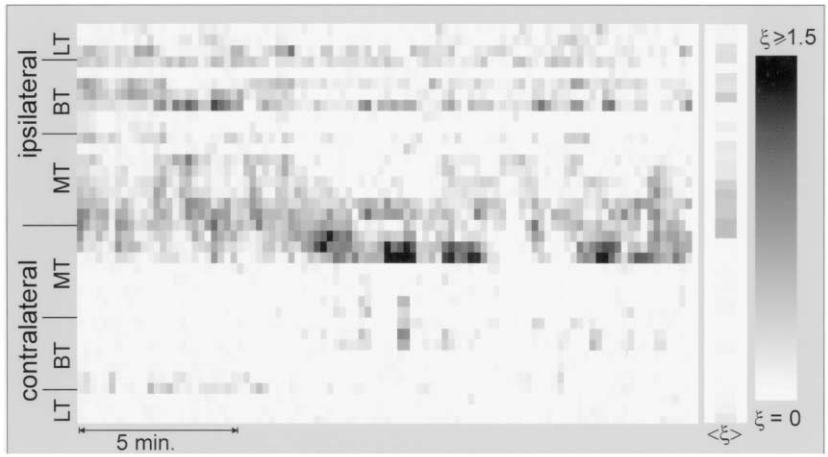


Fig. 4. Values of $\xi$ calculated from an EEG recording (duration: 20 min) of a patient (ID: (e) in Fig. 5). Mean values of $\xi$ are depicted for all channels over time (cf. Fig. 1 for abbreviations of recording regions).

mologous structures, maximum values of $\overline{\xi}$ were found for the mesial temporal recording site in 11 of 17 cases. For the remaining cases, maximum values were found for the ipsilateral basal temporal recording region in five cases and even contralateral to the epileptogenic zone in one case. These cases are marked by asterisks in Fig. 5(b). In no case did the lateral temporal recording sites exhibit maximum values.

## 4. Discussion

In the present study, the measure $\xi$ that aims at discriminating nonlinear deterministic dynamics from linear stochastic dynamics, has been introduced. Values of this measure were calculated from intracranial interictal EEG recordings of patients with postoperatively verified unilateral mesial temporal lobe epilepsy. Summarizing the results, higher values of $\overline{\xi}$ were calculated for the EEGs recorded within the epileptogenic zone compared to those obtained for homologous contralateral structures in all 25 cases. If these findings are interpreted as a correct retrospective lateralization of the epileptogenic zone, it follows that $\xi$ can contribute to a spatial characterization of the epileptogenic process even without the necessity to observe actual seizure activity.

A correct lateralization based on results obtained only from the pair of intrahippocampal depth electrodes requires the a priori knowledge of the definite mesial location of the epileptogenic zone. This knowledge also allows the attribution of the decreasing discriminating power found for the basal and lateral regions to their increasing distance from the epileptogenic zone. However, the investigation whether this information could also be confirmed a posteriori by comparing $\overline{\xi}$ values for different brain regions revealed less discriminative results: maximum $\overline{\xi}$ values were found for the ipsilateral basal region and in one case even contralateral to the epileptogenic zone. Hence, further studies dealing with patients with extra-mesial epilepsies are required to evaluate sensitivity and specificity of the measure $\xi$ for the epileptogenic process.

A high temporal variability of $\xi$ values was found on both short and long time scales. Since recordings were not selected to fulfill standardized conditions, this variability might be attributed to factors such as varying levels of anticonvulsive medication (Lehnertz and Elger, 1997) or changes in vigilance (Fell et al., 1996) that have been shown to affect NTSA-measures calculated from the EEG.

As for any NTSA-measure, the interpretation of absolute values of $\xi$ calculated from EEG time

series remains difficult. Nonzero values of $\xi$ do not provide a sufficient criterion for the detection of nonlinear determinism. On the one hand, nonstationarity causes a rejection of the null hypothesis of the surrogates, which are stationary by construction. The deviation of $\Lambda_{\mathrm{EEG}}(\tau)$ from the surrogates' mean of examples (b) in Figs. 2 and 3 may be explained by the obvious nonstationarities and the surrogates' mean might even exhibit a higher local flow in the reconstructed state space than for the EEG time series, as shown for example (b) in Fig. 3. On the other hand, the rapid

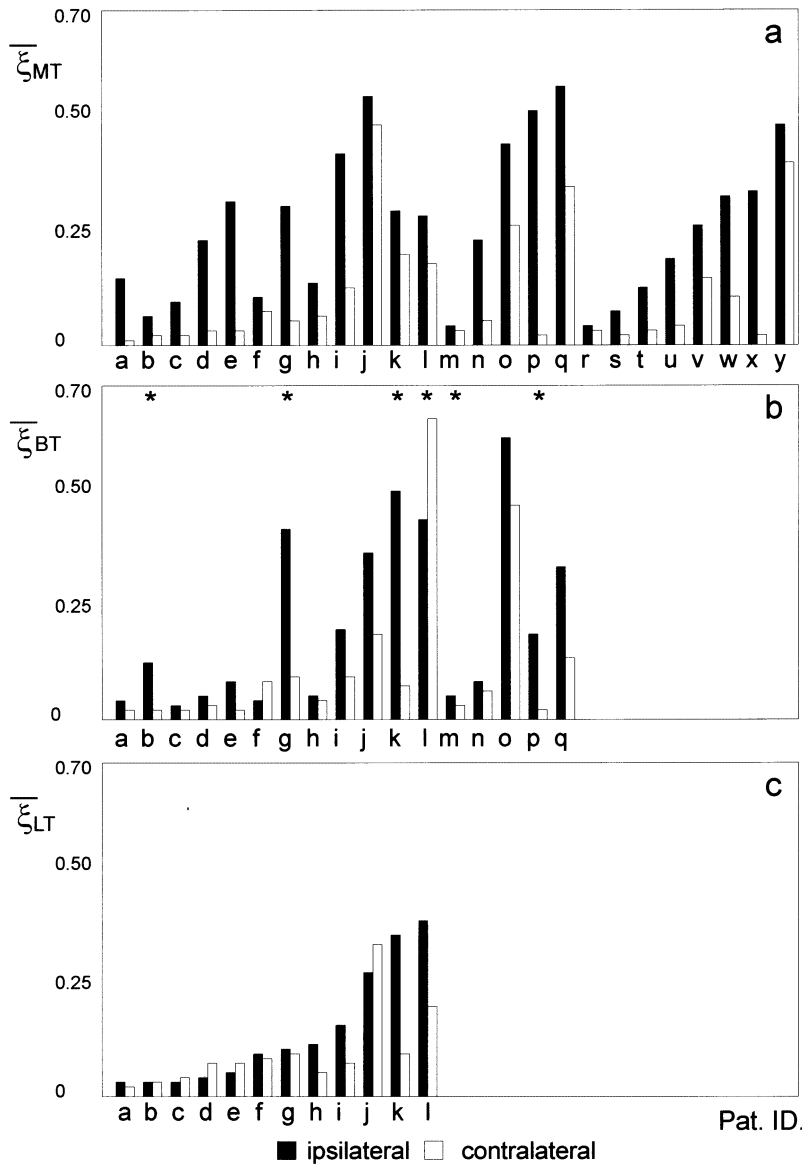


Fig. 5. Mean values $\overline{\xi}$ for all patients (a–y) and recording regions. From top to bottom bars depict results obtained for the mesial temporal, basal temporal and the lateral temporal recording region (cf. Fig. 1). For patients without no symmetrical implantation of subdural strip electrodes (BT or LT), no bars were plotted. For this group, asterisks mark those cases in which maximum $\overline{\xi}$ values were found for non-mesial recording regions.

Table 1
Influence of the side of the epileptogenic zone on differences between homologous recording regions (ANOVA using $F$-tests) and results of discriminant analyses using interhemispheric differences of $\overline{\xi}$ values at the respective recording location[a]

| Recording location | No. of cases | No. of correctly classified cases | $P$-value |
|---|---|---|---|
| MT | 25 | 25 | $<0.001$ |
| BT | 17 | 14 | 0.029 |
| LT | 12 | – | n.s. |

[a] For abbreviations of recording locations cf. Fig. 1. For the basal temporal recording region of Patient c (cf. Fig. 5), higher $\overline{\xi}$ values are obtained on the side of the epileptogenic zone. Nevertheless, due to the smallness of this difference, this individual case was classified as an incorrect lateralization by the discriminant analysis.

decay of the coarse-grained flow average with increasing values of the reconstruction delay might even be considered to indicate nonlinear stochastic dynamics rather than nonlinear deterministic dynamics. However, it might likewise be interpreted as the smearing of deterministic structures by both measurement and dynamical noise from other parts of the neuronal network not included in the EEG measurement. Finally, deterministic dynamics are not necessarily reflected in nonzero values of $\xi$, because the coarse-grained flow average is not able to resolve arbitrarily complicated deterministic dynamics. This holds especially true for time series of finite length and resolution. Despite these limitations, the present findings support the hypothesis that the epileptogenic process induces or enhances nonlinear deterministic structures in the otherwise linear stochastic appearance of brain electrical activity.

To our knowledge, the present investigation is the first attempt to apply a straightforward test for nonlinear determinism to intracranial EEG recordings from patients with epilepsy. If the trend of decreasing $\overline{\xi}$ values with increasing distance to epileptogenic zone obtained intracranially would be extrapolated to the scalp, findings would be in agreement with those of Glass et al. (1993), Palus (1994) and Jeong et al. (1999) obtained from scalp EEG recordings in healthy subjects. Supplementary to previous studies using other measures (Iasemides et al., 1990; Lehnertz and Elger, 1995; Casdagli et al., 1997; Weber et al., 1998), the present study shows nonlinear time series analyses to extract information potentially useful for diagnostic purposes from EEG recordings of seizure free intervals. In theory, each of these measures exploits complementary characteristics of the underlying dynamics. In practice, however, further studies are needed to investigate the degree to which non-redundant information is extracted from the EEG.

## Acknowledgements

We are grateful to Wieland Burr, Kristin Jerger, Florian Mormann and Theoden Netoff for fruitful discussion and valuable comments on earlier versions of this manuscript. This work was supported by the Deutsche Forschungsgemeinschaft.

## Appendix A. State space reconstruction

Assuming a dynamical system can be fully described by $d$ variables $x_1(t), \ldots, x_d(t)$, a geometrical representation of the dynamics in an abstract $d$-dimensional state space can be achieved by constructing a time dependent state vector:

$$v(t) = (x_1(t), \ldots, x_d(t)) \tag{A1}$$

While the system evolves in time, the vector's tip passes through the state space along the so called trajectory. Each state of the system is represented by a point on this trajectory and vice versa. A dynamical system is called deterministic if an unambiguous relationship exists between all present states and their respective future trajectories. Furthermore, for smooth deterministic dynamics, similar present states lead to similar states in the near future. In accordance with these defin-

itions, trajectories generated by smooth deterministic dynamical systems show no self-intersections and nearby segments are aligned, i.e. a deterministic local flow manifests itself in state space. In contrast, no relationship exists between present states and the respective future evolution for stochastic dynamical systems. Hence, nearby trajectory segments intersect each other (cf. Fig. 6) and, in general, show no particular alignment.

In the case of a single scalar time series $y(t)$, measured within a dynamical system by means of a measurement function $g$:

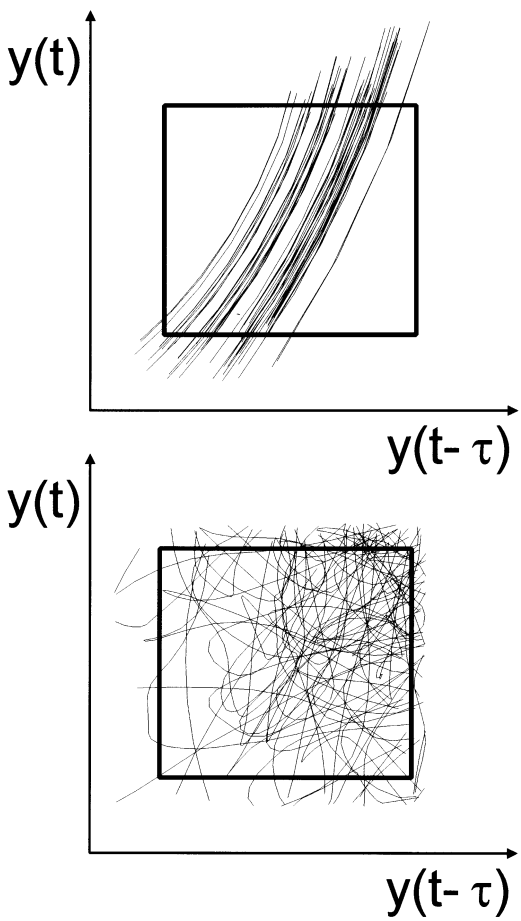


Fig. 6. Schemes of clipped trajectories within a hypercube illustrating different extremes of alignment of adjacent segments. State space was reconstructed using delay coordinates. Upper part: nonlinear deterministic dynamics; lower part: a spaghetti mess of trajectories from a linear stochastic dynamics.

$$y(t) = g(v(t)) \tag{A2}$$

the method of delay-coordinates allows reconstruction of the dynamics in an $m$-dimensional state space using a time delay $\tau$:

$$z(t) = (y(t), y(t-\tau), \ldots, y(t-(m-1)\tau)) \tag{A3}$$

Takens (1981) has shown that for an infinite, continuous time series $y(t)$, a smooth transformation between the genuine trajectory $v(t)$ and reconstructed trajectory $z(t)$ exists for all time delays $\tau$ if the embedding dimension $m$ is chosen as $m \geq 2d+1$. Thus, in principle, all geometrical properties of $v(t)$ are preserved by $z(t)$, including the above mentioned deterministic alignment of nearby trajectory segments. In practice, however, when Eq. (A3) is applied to time series of finite length measured on a system with unknown dynamical properties, the embedding dimension cannot be chosen correctly a priori, since the genuine dimension $d$ is unknown. Furthermore, a good estimate of the underlying dynamics can be obtained only for a limited range of the time delay $\tau$. When the method of delay coordinates is applied to time series measured on a stochastic dynamical system, linear autocorrelations in the time series are sufficient to yield locally preferred directions, i.e. a non-deterministic local flow in the reconstructed state space.

### *A.1. Coarse-grained flow average*

In order to quantify the average degree of alignment of nearby segments of the delay-coordinate trajectory $z(t)$, the state space is divided into $b^m$ non-overlapping rectangular hypercubes, where $b$ denotes the number of hypercubes per phase space axis. If a hypercube with index $j$ is passed $n_j$-times by $z(t)$, for each pass a tangent vector of unit length $v_{k,j}$ $(k = 1, \ldots, n)$ is generated, whose direction is determined by connecting the points where the trajectory enters and leaves the hypercube. Summing up all vectors of passes through hypercube $j$, the resultant vector $V_j$, normalized by the number of passes $n_j$, is:

$$V_j = \frac{1}{n_j} \sum_k v_{k,j} \tag{A4}$$

If the included trajectory segments are aligned, $V_j$ is almost of unit length.

The expectation value $R$ of the vector addition in Eq. (A4) for $n$ vectors of unit length yielded by a random walk process (cf. Kaplan and Glass 1992 and references therein) decreases as $n$ increases as follows:

$$R \propto \frac{1}{\sqrt{n}} \tag{A5}$$

In order to summarize the huge amount of local information, the following average is constructed over all occupied hypercubes:

$$\Lambda = \sum_j \frac{V_j^2 - R^2}{1 - R^2} \tag{A6}$$

$\Lambda$ quantifies the local flow in state space, but is insensitive to whether it reflects determinism or simply preferred directions due to autocorrelations. The method of surrogate data helps to circumvent this uncertainty.

### *A.2. Surrogate data*

To test the null hypothesis that certain values of an NTSA-measure (here $\Lambda > 0$) calculated for $y(t)$ are sufficiently explicable by properties compatible with a linear random process rather than by nonlinear deterministic dynamics, an ensemble of surrogate time series can be generated which share these linear properties, but are otherwise random. Only if the result obtained for the original time series is outside the distribution of the surrogate ensemble at a given level of significance can the null hypothesis be rejected. In this study, iterative amplitude-adjusted surrogates were used (Schreiber and Schmitz, 1996). This type of surrogate time series is constructed using an iterative permutation of the original sample values of $y(t)$, so that the amplitude distribution is maintained by construction. While the phases of the complex Fourier coefficients are randomly shuffled, their amplitudes and with it the power spectrum and therefore linear autocorrelations (Wiener–Khinchin theorem) of the surrogates are practically indistinguishable from those of the original time series (Schreiber and Schmitz, 1996).

## References


Alarcon, G., Binnie, C.D., Elwes, R.D.C., Polkey, C.E., 1995. Power spectrum and intracranial EEG patterns at seizure onset in partial epilepsy. Electroenceph. Clin. Neurophysiol. 94, 326–337.

Alarcon, G., Garcia Seoane, J.J., Binnie, C.D., Martin Miguel, M.C., Juler, J., Polkey, C.E., Elwes, R.D.C., Ortiz Blasco, J.M., 1997. Origin and propagation of interictal discharges in the acute electrocorticogram. Implications for pathophysiology and surgical treatment of temporal lobe epilepsy. Brain 120, 2259–2282.

Babloyantz, A., Destexhe, A., 1986. Low-dimensional chaos in an instance of epilepsy. Proc. Natl. Acad. Sci. USA 83, 3513–3517.

Casdagli, M.C., 1989. Nonlinear prediction of chaotic time series. Phys. D 35, 335–356.

Casdagli, M.C., Iasemides, L.D., Savit, R.S., Gilmore, R.L., Roper, S.N., Sackellares, J.C., 1997. Non-linearity in invasive EEG recordings from patients with temporal lobe epilepsy. Electroenceph. Clin. Neurophysiol. 102, 98–105.

Chang, T., Schiff, S.J., Sauer, T., 1994. Stochastic versus deterministic variability in simple neuronal circuits I. Monosynaptic spinal cord reflexes. Biophys. J. 67, 671–683.

Drake, M.E., Padamadan, H., Newell, S.A., 1998. Interictal quantitative EEG in epilepsy. Seizure 7, 39–42.

Engel, J. Jr, 1993. Surgical Treatment of the Epilepsies. Raven Press, New York, pp. 740–742.

Fell, J., Röschke, J., Mann, K., Schäffner, C., 1996. Discrimination of sleep stages: A comparison of spectral and nonlinear EEG measures. Electroenceph. Clin. Neurophysiol. 98, 401–410.

Frank, G.W., Lookman, T., Nerenberg, M.A.H., Essex, C., Lemieux, J., Blume, W., 1990. Chaotic time series analyses of epileptic seizures. Phys. D 46, 427–438.

Gersch, B., Goddard, G.V., 1970. Epileptic focus localisation: spectral analysis method. Science 169, 701–702.

Glass, L., Kaplan, D.T., Lewis, J.E., 1993. Tests for deterministic dynamics in real world and model neuronal networks. In: Jansen, B.H., Brandt, M.E. (Eds.), Nonlinear Dynamical Analysis of the EEG. World Scientific, Singapore, pp. 233–238.

Iasemides, L.D., Sackellares, J.C., Zaveri, H.P., Williams, W.J., 1990. Phase space topography and the Lyapunov exponent of electrocorticograms in partial seizures. Brain Topogr. 2, 187–201.

Jeong, J., Kim, M.S., Kim, S.Y., 1999. Test for low-dimensional determinism in electroencephalograms. Phys. Rev. E 60, 831–837.

Kantz, H., Schreiber, T., 1995. Dimension estimates and physiological data. Chaos 5, 143–154.

Kantz, H., Schreiber, T., 1997. Non-Linear Time Series Analysis. Cambridge University Press, Cambridge, UK.

Kaplan, D.T., 1994. Exceptional events as evidence for determinism. Phys. D 73, 38–48.

Kaplan, D.T., Glass, L., 1992. Direct test for determinism in a time series. Phys. Rev. Lett. 68, 427–430.

Lehnertz, K., Elger, C.E., 1995. Spatio-temporal dynamics of the primary epileptogenic area in temporal lobe epilepsy characterized by neuronal complexity loss. Electroenceph. Clin. Neurophysiol. 95, 108–117.

Lehnertz, K., Elger, C.E., 1997. Neuronal complexity loss in temporal lobe epilepsy: effects of carbamazepine on the dynamics of the epileptogenic focus. Electroenceph. Clin. Neurophysiol. 103, 376–380.

Lopes da Silva, F.H., Storm van Leeuwen, W., Rémond, A. (Eds.), 1986. Handbook of Electroencephalography and Clinical Neurophysiology, vol. 2. Elsevier, Amsterdam.

Lüders, H.O., Awad, I., 1991. Conceptual considerations. In: Lüders, H.O. (Ed.), Epilepsy Surgery. Raven Press, New York, pp. 51–62.

Marciani, M.G., Stefanini, N., Stefanini, F., Maschio, M.C.E., Gigli, G.L., Bernardi, G., Caltagirone, C., 1992. Lateralization of the epileptogenic focus by computerized EEG study and neuropsychological evaluation. Int. J. Neurosci. 66, 53–60.

Nuwer, M.R., 1988. Frequency analysis and topographic mapping of EEG and evoked potentials in epilepsy. Electroenceph. Clin. Neurophysiol. 69, 118–126.

Osborne, A.R., Provenzale, A., 1989. A finite correlation dimension for stochastic systems with power-law spectra. Phys. D 35, 357–381.

Palus, M., 1994. Nonlinearity in normal human EEG: cycles, temporal asymmetry, nonstationarity and randomness, not chaos. Biol. Cybern. 75, 389–396.

Panet-Raymond, D., Gotman, J., 1990. Asymmetry in delta activity in patients with focal epilepsy. Electroenceph. Clin. Neurophysiol. 75, 474–481.

Pijn, J.P., van Neerven, J., Noest, A., Lopes da Silva, F., 1991. Chaos or noise in EEG signals; dependence on state and brain site. Electroenceph. Clin. Neurophysiol. 79, 371–381.

Rapp, P.E., Albano, A.M., Schmah, T.I., Farwell, L.A., 1993. Filtered noise can mimic low dimensional chaotic attractors. Phys. Rev. E 47, 2289–2297.

Rombouts, S.A.R.B., Keunen, R.W.M., Stam, C.J., 1995. Investigation of nonlinear structure in multichannel EEG. Phys. Lett. A 202, 352–358.

Salvino, L.W., Cawley, R., 1994. Smoothness implies determinism: A method to detect it in time series. Phys. Rev. Lett. 73, 1091–1094.

Schiff, S.J., Chang, T., 1992. Differentiation of linearly correlated noise from chaos in a biological system using surrogate data. Biol. Cybern. 67, 387–393.

Schiff, S.J., Jerger, K., Chang, T., Sauer, T., Aitken, P.G., 1994. Stochastic versus deterministic variability in simple neuronal circuits II. Hippocampal slice. Biophys. J. 67, 684–691.

Schreiber, T., 2000. Is nonlinearity evident in time series of brain electrical activity? In: Lehnertz, K., Arnhold, J., Grassberger, P., Elger, C.E. (Eds.), Chaos in Brain? World Scientific, Singapore, pp. 13–22.

Schreiber, T., Schmitz, A., 1996. Improved surrogate data for nonlinearity tests. Phys. Rev. Lett. 77, 635–638.

Schuster, H.G., 1989. Deterministic Chaos, second ed. VCH, Weinheim.

So, P., Ott, E., Sauer, T., Gluckman, B.C., Grebogi, C., Schiff, S.J., 1997. Extracting unstable periodic orbits from chaotic time series data. Phys. Rev. E 55, 5398–5417.

So, P., Francis, T.J., Netoff, T.I., Gluckman, B.C., Schiff, S.J., 1998. Periodic orbits: A new language for neuronal dynamics. Biophys. J. 74, 2776–2785.

Spencer, S.S., So, N.K., Engel, J. Jr, Williamson, P.D., Levesque, M.F., Spencer, D.D., 1993. Depth electrodes. In: Engel, J. Jr (Ed.), Surgical Treatment of the Epilepsies. Raven Press, New York, pp. 359–376.

Takens, F., 1981. Detecting strange attractors in turbulence. In: Rand, D.A., Young, L.S. (Eds.), Dynamical Systems and Turbulence. Lecture Notes on Mathematics, vol. 898. Springer, New York, pp. 366–381.

Theiler, J., 1995. On the evidence for low-dimensional chaos in an epileptic electroencephalogram. Phys. Lett. A 196, 335–341.

Theiler, J., Rapp, P.E., 1996. Re-examination of the evidence for low-dimensional, nonlinear structure in the human electroencephalogram. Electroenceph. Clin. Neurophysiol. 98, 213–222.

Theiler, J., Eubank, St., Longtin, A., Galdrikian, B., Farmer, J.D., 1992. Testing for nonlinearity in time series: the method of surrogate data. Phys. D 58, 77–94.

Van Roost, D., Solymosi, L., Schramm, J., van Oosterwyck, B., Elger, C.E., 1998. Depth electrode implantation in the length axis of the hippocampus for the presurgical evaluation of the medial temporal lobe epilepsy: A computed tomography-based stereotactic insertion technique and its accuracy. Neurosurgery 43, 819–826.

Wayland, R., Bromley, D., Pickett, D., Passamante, A., 1993. Recognizing determinism in a time series. Phys. Rev. Lett. 70, 580–582.

Weber, B., Lehnertz, K., Elger, C.E., Wieser, H.G., 1998. Neuronal complexity loss in interictal EEG recorded with foramen ovale electrodes predicts side of primary epileptogenic area in temporal lobe epilepsy: A replication study. Epilepsia 39, 922–927.

Widman, G., Lehnertz, K., Urbach, H., Elger, C.E., 2000. Spatial distribution of neuronal complexity loss in neocortical epilepsies. Epilepsia 41, 811–817.